IOP Conf. Series: Materials Science and Engineering **317** (2018) 012023 doi:10.1088/1757-899X/317/1/012023

Corrosion Effects on the Fatigue Crack Propagation of Giga-Grade Steel and its Heat Affected Zone in pH Buffer Solutions for Automotive Application

H S Lee[1]

[1]Department of Automotive Management Engineering, Joongbu University, Goyang-si, Gyeonggi-do, 10279, South Korea

Abstract. Corrosion fatigue crack propagation test was conducted of giga-grade steel and its heat affected zone in pH buffer solutions, and the results were compared with model predictions. Pure corrosion effect on fatigue crack propagation, particularly, in corrosive environment was evaluated by means of the modified Forman equation. As shown in results, the average corrosion rate determined from the ratio of pure corrosion induced crack length to entire crack length under a cycle load were 0.11 and 0.37 for base metal and heat affected zone, respectively, with load ratio of 0.5, frequency of 0.5 and pH 10.0 environment. These results demonstrate new interpretation methodology for corrosion fatigue crack propagation enabling the pure corrosion effects on the behavior to be determined.

1. Introduction

Recently, the application of ultra-high strength steel sheet has been increasing in the automobile industry to improve the fuel efficiency by reducing weight of the vehicle body [1]. It is very important to analyse the characteristics of corrosion of giga-grade steels developed for this purpose, and to find ways to apply them to actual vehicles. The corrosion resistance characteristic of steel is caused by a thin layer of oxides in particular chromium and iron oxides, and despite a thickness of a few nanometers, this oxide layer is so strong that it effectively isolates the steel from the environment 2-3. Once a layer has formed, the metal has become passivated, and the oxidation or rusting rate would slow down to less than 0.05 mm per year. Unfortunately, this kind of ideal process does not always take place; the oxide layer has been damaged without re-passivation, and the result has been shown serious corrosion [2]. Since many study and chemical applications have been conducted, most of the cases were done in NaCl or acid environments. However, the other cases in chemical industries and power plants deal with alkaline solutions and use giga-grade steels in a broad area of products including transfer pipe, heat exchanger, container, etc. [3]. In this study, the fatigue crack propagation (FCP) and corrosion fatigue crack propagation (CFCP) were investigated by experimentally in air together with pH 7.0 of KH_2PO_4(1%)+Na_2HPO_4(1%)+H_2O(98%) and pH 10.0 of Na_2CO_3(1%)+$Na_2B_4O_7$.10H_2O(1%)+H_2O(98%) environments, respectively. And then, a methodology to evaluate the corrosion effect on fatigue crack propagation in corrosive environment has been established based on the modified Forman equation by using the experimental da/dN–△ K relations and average corrosion rate. The mechanisms of corrosion fatigue crack propagations, together with the pure corrosion effect on the crack propagation thus can be determined by the newly developed scheme.

2. Chemical reaction in corrosive environment

The chemical reactions of giga-grade steel with pH buffer solutions were investigated. Buffer solution of pH 7 is chemically reacted as $KH_2PO_4 + H_2O \rightarrow H_3PO_4 + KOH$ with $PO_4^{3-} + H_2O \rightarrow HPO_4^{2-} + OH^-$. In case of pH 10, it is reacted as $Na_2B_4O_7 + H_2O \rightarrow H_3BO_3 + NaOH$ with $CO_3^{2-} + H_2O \rightarrow HCO_3^- + OH^-$. Both of the processes produce OH^-, and the OH^- ions reacted with Fe^{2+} ions from metal dissolution processes at anodic sites. The formation of anodic sites by disruption of the protective passive film on the metal surface leads to the metal dissolution. The anodic iron dissolution reaction is presented by $Fe \rightarrow Fe^{2+} + 2e$. This is balanced by the cathodic reaction of oxygen on the adjacent surface as $O^2 + H_2O+2e \rightarrow 2OH^-$. Due to the continuing Fe dissolution, an excess of positive ions Fe^{2+} is accumulated in the anodic area, which are necessary for the growth of pitting. In addition, a presence of Na^+ ions affects to the acceleration of anodic dissolution especially at the tip of the crack produced by pitting as an anode despite of the surface in non-pitting region as a cathode because the Na^+ ions act as a catalyst in chemical ionization of $Fe(OH)_2$ as $Fe(OH)_2 + 2Na^+ \rightarrow Fe^{2+} + 2NaOH$. Consequently, the larger and deeper pits which formed on the surface of the specimens exposed in pH buffer solutions. And the presence of OH^- ions affects to the hydrolysis as $Fe^{2+} + 2OH^- \rightarrow Fe(OH)_2$ and also to the rust formation as $4Fe(OH)_2 + 2H_2O + O_2 \rightarrow 4Fe(OH)_3$.

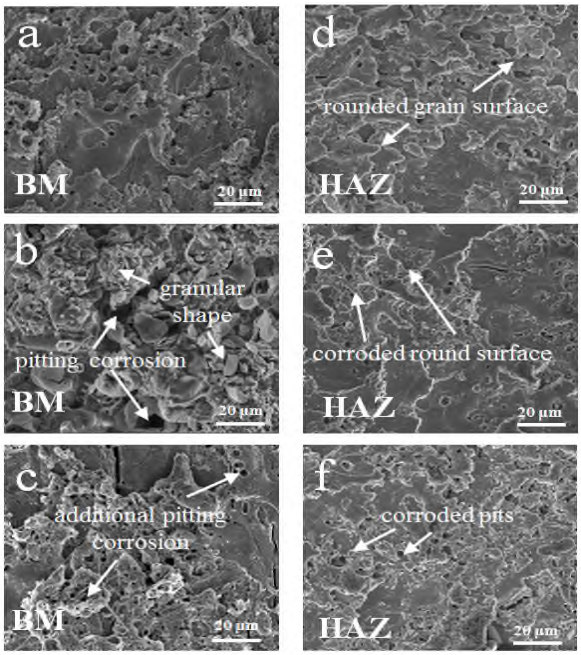

Figure 1. SEM observations of giga-grade steel immersed in buffer solutions of pH 7 and pH 10 for 7 days; (a) BM in air, (b) BM in pH 7.0, (c) BM in pH 10.0, (d) HAZ in air, (e) HAZ in pH 7.0, (f) HAZ in pH 10.0.

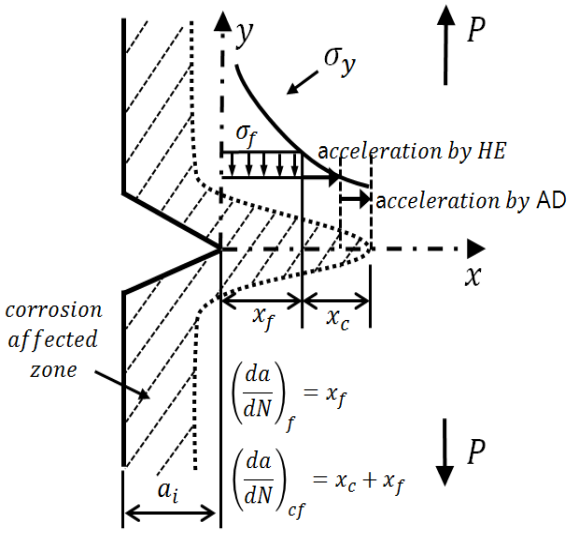

Figure 2. Schematic diagram showing the corrosion fatigue crack propagation process [4].

Based on these chemical reaction mechanisms, base material (BM) and heat affected zone (HAZ) of giga-grade steel were prepared for experiment. Before commencement of the corrosion fatigue test, specimens of giga-grade steel were in buffer solutions of pH 7 and pH 10 for 7 days resulting in pre-chemical reactions and the microstructures obtained at this stage are presented in figure 1. Figures 1a, 1b and 1c show the corroded surface of BM in air, pH 7 and pH 10 environments, respectively. Pitting corrosions were presented with rust formed granular shape on the surface of specimen in pH 7

environment and additional pitting corrosions were evolved on the granular shape surface. Figures 1d, 1e and 1f show the corroded surface of HAZ in air, pH 7 and pH 10 environments, respectively. HAZ had more rounded grain surface in air environment compare to the BM in figure 2d. The round grain surface was corroded in pH 7 in figure 1e and severely corroded pits were evolved in pH 10 environment in figure 1f.

3. Corrosion fatigue crack propagation

It is kwon that the corrosion fatigue crack propagation (CFCP) is caused by the combination of corrosion damage and relative slip of the metal at the crack tip under cyclic loading. This process is controlled by the three major mechanisms: relative slip of the metal at the crack tip, the bare surface corrosion of the fractured material elements and the crack closure. The corrosion in the CFCP process may occur mainly on the bare surface after the material elements are fractured [4]. In aqueous environment, two possible mechanisms are associated with the corrosion damage on the CFCP process: anodic dissolution (AD) at the crack tip, and hydrogen penetration by AD into the material elements resulting in hydrogen embrittlement (HE). In consequence, both AD and HE lead out the acceleration of crack propagation where it is not the case of air environment [5]. As shown in figure 2, as a state of pre-cracked length of a_i in the specimen, a material element exposing crack tip may be fractured by applied load, P when the level of stress at the crack tip reaches failure strength of the material. Only considering the stress effect without any corrosion such as FCP in a cyclic loading hysteresis, following processes occur: crack opening by increasing load - crack propagation due to fracture of the material element at crack tip - crack closing by decreasing load - crack opening [6]. However, in a corrosive environment, CFCP may occur by the processes: crack opening by increasing load - longer crack propagation due to decrease of failure strength by HE - additional crack propagation with blunting at the crack tip by AD - crack closing by decreasing load - crack opening [4]. Herein, the rate of fatigue crack propagation (FCP) is given by $\left(da/dN\right)_f = x_f$, where x_f is the length of crack propagation in a loading cycle. Meanwhile, the CFCP will be accelerated by the two different mechanisms, HE and AD in the corrosive environment as mentioned before. Total amount of the CFCP length in a cyclic load therefore gives the CFCP rate as:

$$\left(\frac{da}{dN}\right)_{cf} = x_c + x_f \tag{1}$$

In here, x_c is the length of additional crack propagation in a cycle due to the corrosion effect. Although Wang's CFCP model [4] is pretty rare in corrosion fatigue study, the equation has still some limitation on fitting the rapid propagation region III such as the changing slope according to varying load conditions due to the fixed exponent constant, in Paris model. Also, the effect of load frequency was not considered in the equation properly. Therefore, an adequate model which can describe both the FCP and the CFCP behaviours was required to reveal the significance of the parameters related to environmental effects. In order to identify the pure corrosion effect on fatigue crack propagation in corrosive environment, the average corrosion rate (C_a) during one loading period T is considered as follows

$$C_a = \frac{1}{T}\frac{x_c}{x_c + x_f} = f\frac{x_c}{x_c + x_f} \tag{2}$$

And then, the x_c term can be rearranged as $x_c = C_a x_f / \left(f - C_a\right)$.

Generally, fatigue crack propagation behaviour of a material has been described by the FCP rate, da/dN against the stress intensity factor range (SIFR), ΔK. Among the several models, the modified Forman equation enables the FCP behaviour to be modeled within the full range of crack propagation such

as an initial crack propagation of threshold region (Region I), stable crack growth (Region II), and fast fracture region with rapid-unstable crack growth (Region III). The material's characteristics of FCP behaviour by considering the modified Forman equation give the formulation:

$$\left(\frac{da}{dN}\right)_{fat} = x_f = \frac{M\left(\Delta K - \Delta K_{th}\right)^N}{\left(1-R\right)K_{crit} - \Delta K} \tag{3}$$

where, two parameters, M and N and ΔK_{th} value at a certain level of SIFR were selected as the characteristics of the FCP behaviour. M and N were indicating the intercept of da/dN -axis and the slope of the curve in linear region, and the subscript *th* and *crit* indicates threshold value and critical value of SIFR, respectively.

Substituting (2) and (3) into equation (1), a CFCP model for determination of corrosion effect can be expressed:

$$\left(\frac{da}{dN}\right)_{cf} = x_c + x_f = \frac{C_a x_f}{f - C_a} + x_f = \left(1 + \frac{C_a}{f - C_a}\right)\left[\frac{M\left(\Delta K - \Delta K_{th}\right)^N}{\left(1-R\right)K_{crit} - \Delta K}\right] \tag{4}$$

In here, x_f and C_a in x_c term can be obtained from the results of air condition, and corresponding pH and loading conditions, respectively. By comparing the FCP and CFCP behaviours of giga-grade steel in air and pH buffer solutions such as pH 7.0 and pH 10.0, and consequently the corrosion effects in alkaline environment therefore can be analysed.

Table 1. Thermal cycles for HAZ simulation.

Method	Preheat temp. (°C)	Peak temp. (°C)	Heating rate (°C/s)	Cooling rate (°C/s)	Cycles and heat input
GTAW	25	410	258	5	1 cycle (16kJ/cm)

Experiments were conducted by using the giga-grade steel as a base metal (BM) and heat affected zone (HAZ) to investigate FCP and CFCP of the materials. Table 1 shows the welding cycles to develop the HAZ with relevant temperature cycle which was calculated by the Rosenthal equation for a thick plate [7] as follows:

$$T_t - T_0 = \frac{q/v}{2\pi\lambda t}\exp\left(-\frac{r^2}{4bt}\right) \tag{5}$$

where T_t is the temperature (K), T_0 is the pre-heat temperature, q/v is the heat input (kJ/cm), λ is the thermal conductivity of giga-grade steel (J/msK), t is the time, b is the thermal diffusivity of giga-grade steel (m^2/s), and r is the radial distance from the heat source. In this work, the HAZ was simulated for single-pass welding by using gas Tungsten arc welding (GTAW). A three-point single edge notched bending (3-SENB) fixture and specimens were used in the FCP and CFCP test (ISO 11782-2). A 6-mm notch was produced on every specimen, followed by formation of a pre-crack at the tip of the notch under cyclic fatigue load with load ratios of 0.1, 0.3, 0.5 and load frequencies of 0.1, 0.3, 0.5. FCP and CFCP tests were conducted at room temperature with a 50 KN capacity universal testing machine. As mentioned previously, three levels of the load ratio (R) and the frequency (f), respectively, 0.1, 0.3 and 0.5, were considered. In addition, CFCP test was conducted by using the 7 days immersed specimens in the same environment condition. In alkaline environment, the corrosion resistance of material is generally reduced by the hydrogen embrittlement. The hydrogen embrittlement is due to the chemical absorption and molecular dissociation which results in the formation of atomic hydrogen, H^+. The atomic hydrogen migrates to pitting root regions of high stress concentration. The absorption of the hydrogen ions into the

pitting root as a crack tip, through a dislocation motion [8] or attracting by the hydrostatic stress gradients [9], promotes embrittlement of the crack tip material. Microstructures of BM and HAZ in air and pH buffer solutions are shown in figure 3. Compare to the air condition in figures 3a and 3d, pitting corrosion evolution aspects are shown in figures 3b and 3c for BM and figures 3e and 3f for HAZ. The corroded pits were produced with narrow hole-shape in pH 7.0, and enlarged corroded pits were generated in pH 10.0. Overall, faster corrosion evolution occurred in HAZ than BM. Corroded pits occurred mainly in the presence of hydrogen and oxide contained solutions. Hydrogen and oxide ions facilitated a local breakdown of the passive layer, especially imperfections in the surface. The root of the corroded pit played an additional notch effect, so stress concentration was arisen in the near of the root tip.

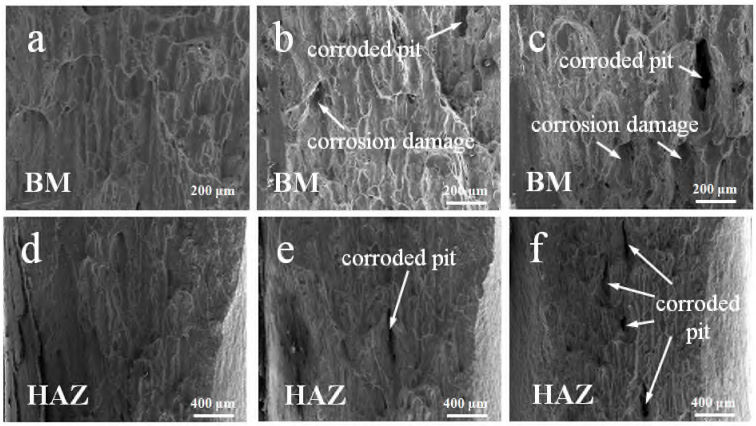

Figure 3. SEM observations of giga-grade steel at fractured section after FCP and CFCP tests; (a) BM in air, (b) BM in pH 7.0, (c) BM in pH 10.0, (d) HAZ in air, (e) HAZ in pH 7.0, (f) HAZ in pH 10.0.

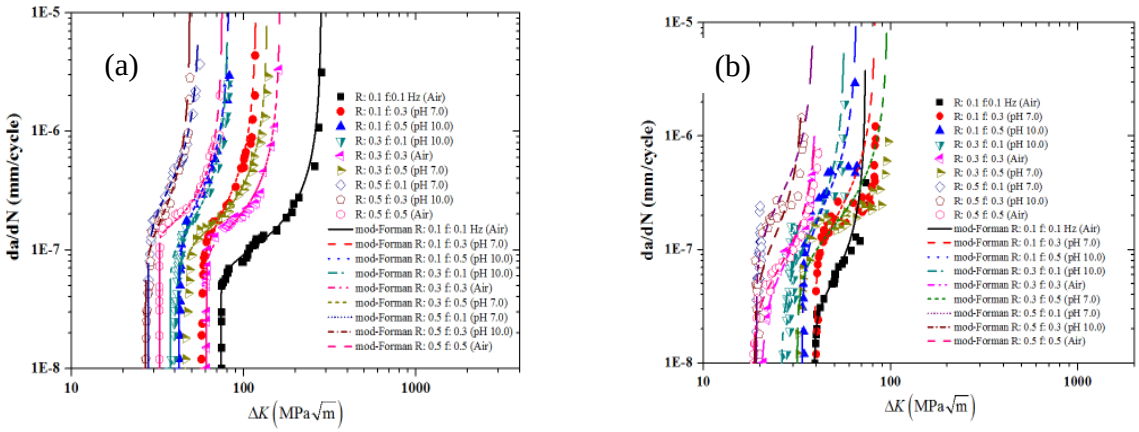

Figure 4. Fatigue and corrosion fatigue crack propagation behaviors of giga-grade grade steel under several environment-loading conditions; (a) BM in air, pH 7.0 and pH 10.0, (b) HAZ in air, pH 7.0 and pH 10.0.

In order to obtain the fatigue parameters of M and N and ΔK_{th} value in a CFCP model of (4), da/dN and SIFR relations of BM and HAZ were examined and the FCP and CFCP rates for the SIFR are shown in figure 4. As can be seen, the modified Forman model demonstrates the whole region of FCP and CFCP behaviours, specifically, regions I, II and III. CFCP rates of the pH buffer solutions were more rapid than the FCPRs in air. And also threshold SIFR values of pH buffer solutions are lower than in air environment.

This is caused by the pitting corrosion cracking which occurs in a corrosive environment due to the stress concentration with the corroded shape and thus a shorter crack propagation path. By using the newly suggested scheme, the average corrosion rates (Ca) in CFCP of BM and HAZ were calculated and the results are expressed in figure 5. As shown in results, more severe corrosion effects were examined in pH 10.0 with higher Ca values than pH 7.0 for both BM and HAZ. In addition, rapid increasing of Ca was found in HAZ while the monotonous increment in BM. It reveals that HAZ is more sensitive to corrosion environment than BM about three times in R=f=0.5 and indicating that thermal damage on the surface of HAZ makes the corrosion solution easy to penetrate. In maximum value of R=f=0.5, more than 30% of the entire crack length is due to the pure corrosion in HAZ of pH 10.0 condition.

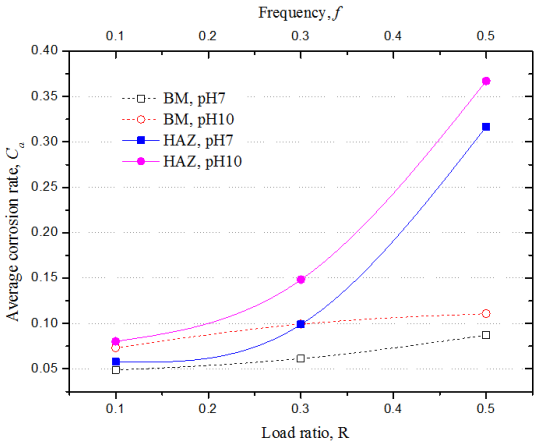

Figure 5. Average corrosion rate against the load ratio with frequency of R=*f*=0.1, R=*f*=0.3 and R=*f*=0.5.

4. Conclusions

Fatigue and corrosion fatigue crack propagation behaviours of giga-grade steel and its HAZ were investigated under several cyclic loads in alkaline solutions. Not only the fatigue crack propagation in such conditions but the corrosion effects on the behaviour were evaluated in terms of the average corrosion rate with modified Forman equation. The new CFCP scheme enabled the determination of length ratio of crack due to the pure corrosion to the entire crack length during CFCP. The HAZ of giga-grade steel showed higher value of the average corrosion rate than the BM about three times in maximum. The calculated maximum crack propagation length ratio against the total crack propagation length due to the pure corrosion during CFCP process was about 0.37 in HAZ of pH 10.0 and R=*f*=0.5. Based on the chemical reaction analysis in corrosion environment, experimentally measured CFPC behaviours together with model predictions present new interpretation methodology to determine the crack propagation length by pure corrosion effects on the fatigue crack propagation in alkaline solutions.

References

[1] Kim H, Choi H, Lim J and Cho Y 2011 *Proc. Spring Conf. on The Korean Society of Automotive Engineers*, p 1877.
[2] Chen G, Duquette D 1992 *Metal. Trans. A.* **23** 1563.
[3] Salih S, El-Masri A and Baraka A 2001 *J. Mater. Sci.* **36** 2547.
[4] Wang R 2008 *Int. J. Fatigue* **30** 1376.
[5] Ruiz J and Elices M 1996 *Corros. Sci.* **38** 1815.
[6] Zheng X and Hirt M 1983 *Eng. Fract. Mech.* **18** 965.
[7] Easterling K 1983 *Introduction to the Physical Metallurgy of Welding* (Butterworth).
[8] Henaff G, Petit J and Bouchet B 1992 *Int. J. Fatigue* **14** 211.
[9] Ellyin F and Wu J 1994 *Acta Metall. Mater.* **42** 2709.